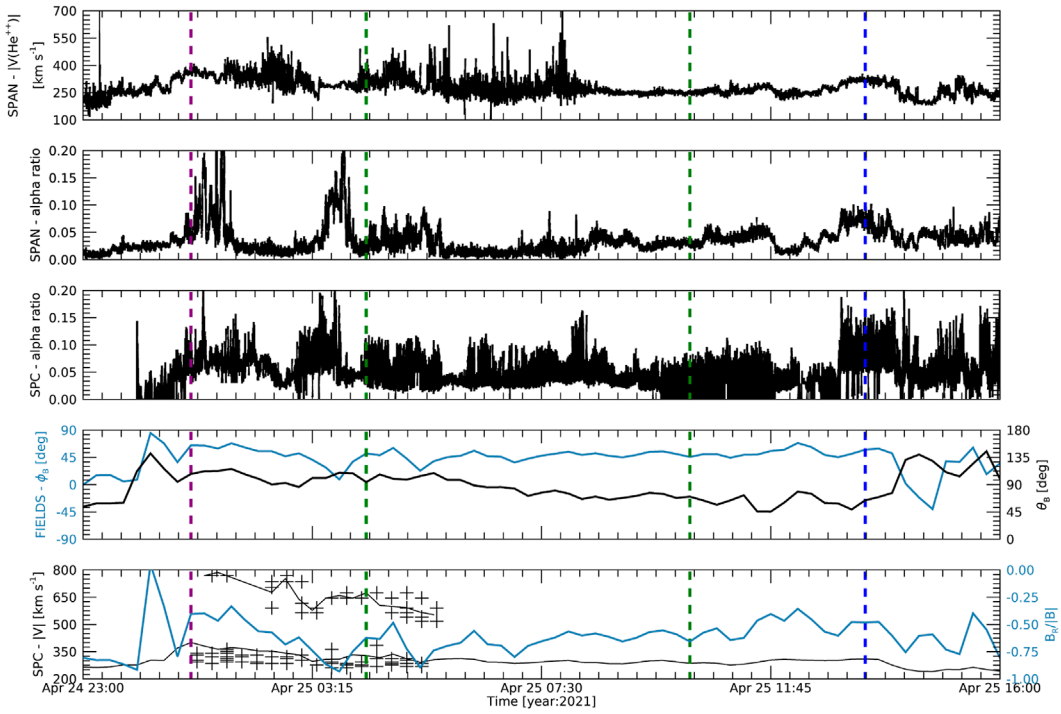

FIGURE 4
82-s time series of the alpha speed (*first* panel) and the alpha ratios measured by SPAN (*second* panel) and SPC (*third* panel) compared with the 15-min time series of the magnetic field direction by FIELDS (ϕ_B shown in *black* and θ_B in *blue*); the $B_R/|B|$ ratio (in *blue*) and SPC-$|V|$ (in *black*). In the *bottom* panel, overplot, we marked the VDF maxima, *first* and *second* peaks, with *black* +. The vertical dash lines correspond to the arrival of the *first* structure (shown in *purple*), the constant speed region (delimited by two *green* lines), and the *second* structure at 310 km s^{-1} (in *blue*). During this period, the flow is fully captured by the SPC sensor and partially by SPAN. Still, both instruments observed speed and alpha ratio enhancements due to the arrival of prominence material.

4 Remote-sensing observations

The remote-sensing observations (from both spacecraft SolO and STEREO-A) show that the eruption occurred in two phases. The first one, a smaller outburst, began in the more southerly part of the prominence around 2021 April 23 at 21:25 UT, and the second, characterized by a substantial eruption, originated from the more northerly part of the prominence around 2021 April 24 at 02:32 UT. It is impossible to say from our observations whether these individual features seen in the EUV and in coronograph observations are really two distinct events or part of a single, more complex one.

For the sake of clarity in the text, we refer to the earlier, smaller outburst as the first eruption and the latter, substantial one, as the second eruption. As these features propagated into the field of view of the several heliospheric imagers we used in this study, they began to become less distinct. Moreover, by the time they reach the PSP spacecraft, they can no longer be distinguished as completely separate events.

During the event, the eruptions propagated to the backside of the Sun from the SDO point of view. In Figure 5, we show the modeled background magnetic field (see Section 2) in different views combined with FSI 304 Å images of the Sun. We note that the model is based on SDO/HMI data from the previous visibility of this region, so there is some uncertainty in the boundary conditions. Assuming that the general magnetic configuration is preserved, the model gives insight into the background magnetic field configuration on 2021 April 23–24. The *top* panels show the magnetic field configuration from the solar North Pole. The *bottom* panels are from PSP (*left*) and SolO (*right*) points of view.

In Figure 5, we also show several open (*gray*), closed (*red*), and short, low-lying (*yellow*) magnetic field lines obtained with the MAS model. *Purple*, *green*, and *blue* colored lines are related to the different structures tracked from the Sun to PSP following Figures 2, 3. These lines originate close to the boundary between open and closed field lines (see Figure 5 *bottom left* panel). The *top right* and *bottom left panels* of Figure 5 show these field lines bending forward from the solar back-side toward the front-side and also toward the solar equator. The low-lying lines barely stick out behind the limb in the *bottom right* perspective and are roughly at the same solar latitude as the erupting filaments (−25 to −45°).

The magnetic field model results predict a scenario in which both eruptions strongly interact with their surroundings. It also predicts the possible filament source region close to the boundaries between open and closed field lines. At the source region, the eruptions are expected to encounter a domain where the magnetic field is complicated, while at farther distances from the Sun, the structures are embedded in regions dominated by open magnetic field lines. In this case, the results also suggest the eruptions being deflected toward the ecliptic plane.

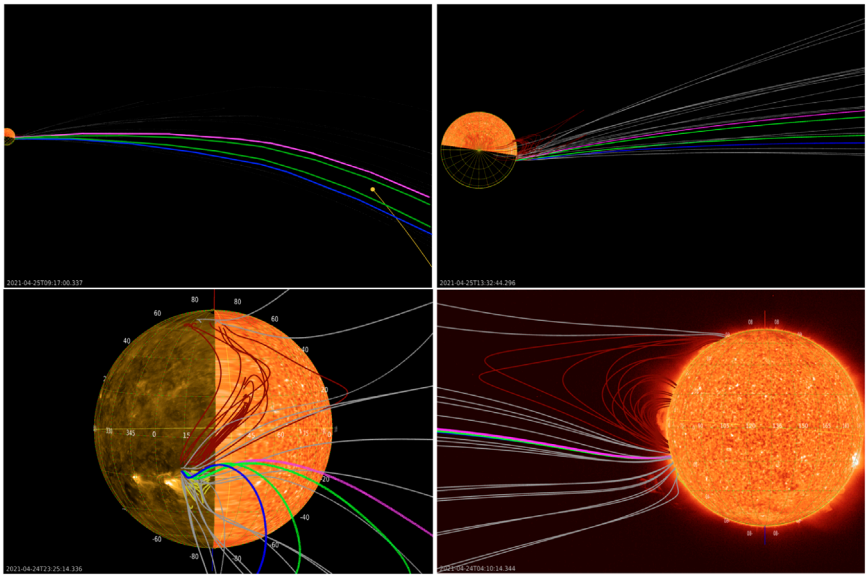

FIGURE 5
Different views of the MAS model field lines with several open (*gray*), close (*red*), and short, low-lying (*yellow*) magnetic field lines with the Sun at 304 Å as seen by FSI. The *top* panels are views down on the solar North Pole, while the *bottom* panels correspond to PSP *left* and SolO (*right*) perspectives. *Purple*, *green*, and *blue* fields are open and connect to the PSP orbit on 2021 April 25 at 01:15 (*first* transient), 04:15, 10:15 (both related to the constant speed patch), and 13:30 (*second* transient) UT (same as in Figures 2, 3). In the *top left* view, the bundle of magnetic field lines moves upward in time with the solar rotation with the PSP trajectory shown as a yellow line ending in a dot. PSP was moving toward the Sun, first crossing the *purple* field line. In the *bottom left* panel, we also include the Sun SDO/AIA 174 Å image on 2021 April 16 at 09:55 UT to illustrate the Sun from the backside as seen from SolO.

4.1 Inner corona

The FSI telescope of EUI, on board SolO, imaged prominence in its 304 Å passband, near the South East limb (from SolO perspective) beginning early on 2021 April 22, as shown in Figure 6 and the accompanying animation. By 2021 April 23, 18:10 UT, this prominence grew into a full arch spanning position angles 120°–135° east from solar north. The first small eruption was seen beginning on 2021 April 23 at 21:25 UT, and the larger part of the prominence, the second eruption, began to untwist and erupted on 2021 April 24 at 02:32 UT.

Both eruptions were also seen in the FSI 174 Å channel. They initially travel (presumably confined by the local magnetic field structures in the corona) strongly non-radially toward decreasing position angles (i.e., northward). Although an FSI data gap (from 03:54 to 06:01 UT) interrupts the observations of the eruption's final lift-off, the eruption was observed and followed at 304 Å reaching 2.7 $R_\odot$ at position angle 110° from the solar disc center on 2021 April 24 at 07:32 UT.

Even though the eruptions originated on the backside of the Sun relative to STEREO-A, they were also visible in the 304 Å channel of EUVI above heights of 1.3 $R_\odot$. Their trajectory in the middle corona was difficult to track due to the severe compression of the EUVI extended field of view. However, the data were nonetheless sufficient to reconstruct the 3D position of the erupting structure using triangulation via epipolar geometry (see Inhester, 2006) with the *scc_measure.pro* program in the *SolarSoft IDL* (Freeland and Handy, 1998) software package. From this, we conclude that the second eruption's initial longitude is around −175° ± 5°, consistent with the magnetic field reconstructions discussed in Section 2. The same reconstruction put the initial eruption around a latitude of about −25°, moving progressively northward to −15°, consistent with the behavior visible across our several remote-sensing observations, although it was difficult to localize due to its extended nature.

4.2 Middle and outer corona

With the prominence erupting behind the limb from the perspective of the STEREO-A spacecraft, there was a subtle signal visible in the COR1 and plainly visible in COR2 coronagraphs. In Figure 7, we show snapshots of these structures. The first had the appearance of an extended loop just to the south of the equatorial plane (Figure 7A) that started to appear early hours on 2021 April 24. The loop was rapidly followed by a faint blob in the equatorial plane (Figures 7B, C) with some vague flux-rope-like structure.

Around 2021 April 24 at 08:00 UT, a CME with the visual characteristics of a small flux-rope entered the COR2 field of view and propagated across it over the course of about 8 h (Figures 7C–E). The structure is defined by the overlap of a circular cross-section feature and a claw-like structure behind it. The first structure we take to be the flux-rope body, while the second one is the CME legs along the line of sight. The rest of the front of the CME body is visible to the sides of the circular cross-section structure. After the CME leaves the field of view, there are a number of small blobs and outflows propagating outward from a similar latitude (Figure 7F).